Journal of Quality Measurement and Analysis
Jurnal Pengukuran Kualiti dan Analisis

JQMA 11(1) 2015, 19-31

STABILITY ANALYSIS OF UNSTEADY THREE-DIMENSIONAL VISCOUS FLOW OVER A PERMEABLE STRETCHING/SHRINKING SURFACE

(Analisis Kestabilan bagi Aliran Likat Tiga Matra tak Mantap terhadap Permukaan Telap Meregang/Mengecut)

EZAD HAFIDZ HAFIDZUDDIN[1], ROSLINDA NAZAR[1], NORIHAN MD ARIFIN[2] & IOAN POP[3]

ABSTRACT

In this paper, a theoretical and numerical study on the unsteady three-dimensional boundary layer flow of a viscous fluid past a permeable stretching/shrinking sheet is considered. Similarity transformation is used to reduce the governing system of nonlinear partial differential equations into a system of ordinary differential equations. These equations are then solved numerically by using the "bvp4c" function in MATLAB. The effects of the governing parameters, namely the unsteadiness parameter, the stretching/shrinking parameter, the suction parameter and the ratio of the surface velocity gradients on the skin friction coefficients, as well as the velocity profiles are presented and discussed. Multiple solutions are found for a certain range of the governing parameters. Stability analysis has been performed to determine which solution is stable and physically realisable.

Keywords: boundary layer; dual solutions; stability analysis; stretching/shrinking sheet; three-dimensional unsteady flow

ABSTRAK

Dalam makalah ini, kajian secara teori dan berangka telah dilakukan bagi aliran lapisan sempadan tiga matra tak mantap bagi bendalir likat melepasi helaian telap meregang/mengecut. Penjelmaan keserupaan digunakan bagi menurunkan sistem menakluk persamaan pembezaan separa tak linear kepada sistem persamaan pembezaan biasa. Persamaan ini kemudiannya diselesaikan secara berangka dengan menggunakan fungsi "bvp4c" dalam perisian MATLAB. Kesan-kesan parameter menakluk, iaitu parameter ketidakmantapan, parameter meregang/mengecut, parameter sedutan dan nisbah kecerunan halaju permukaan terhadap pekali geseran kulit dan profil halaju dibentang dan dibincangkan. Penyelesaian berganda ditemui bagi julat tertentu parameter menakluk. Analisis kestabilan dilakukan bagi menentukan penyelesaian manakah yang stabil dan memberi makna secara fizikal.

Kata kunci: lapisan sempadan; penyelesaian dual; analisis kestabilan; helaian meregang/mengecut; aliran tak mantap tiga matra

1. Introduction

The study of viscous flow and heat transfer due to a stretching sheet has many applications in industrial and manufacturing processes, such as in extrusion, wire drawing, hot rolling and others. Sakiadis (1961a, 1961b) was the first to consider the problem of boundary layer flow over a moving surface. Later, his work is verified by Tsou *et al*. (1967) and extended by Crane (1970) to a stretching plate. McLeod and Rajagopal (1987) discussed the uniqueness of the exact analytical solution presented by Crane (1970), while Gupta and Gupta (1977) extended Crane's work by investigating the effect of heat and mass transfer over a stretching sheet subject to suction or blowing. The problem in Crane (1970) was extended by Wang (1984) to a three-dimensional flow due to a stretching flat surface. More studies regarding flow over a stretching sheet or surface can be found in the literature, such as those by Banks (1983), Rajagopal *et al*. (1984), Chen and Char (1988), Magyari and Keller (1999, 2000) and very recently by Nadeem *et al*. (2014), Bhattacharyya and Layek (2014) and Mabood *et al*. (2015), among others.

Recently, the study of flow due to a shrinking sheet, where the velocity of the boundary is moving towards a fixed point, have become significantly important in the industry. This new type of flow is essentially a backward flow, as described by Goldstein (2006). Miklavcic and Wang (2006) were the first to investigate the viscous flow over a shrinking sheet, followed by Fang *et al*. (2009), who studied the viscous flow over an unsteady shrinking sheet with mass transfer. These authors have shown that from physical point of view, vorticity of the shrinking sheet is not confined within a boundary layer, and the flow is unlikely to exist unless adequate suction on the boundary is imposed. Later, the study regarding shrinking sheet was extended and investigated for various types of fluid and physical properties. On the other hand, Hayat *et al*. (2009) investigated the three-dimentional rotating flow induced by a shrinking sheet for suction, while Aman and Ishak (2010) studied the flow and heat transfer over a permeable shrinking sheet with partial slip. Recently, Rohni *et al*. (2014) considered the flow and heat transfer at a stagnation-point over an exponentially shrinking vertical sheet with suction, while Rahman *et al*. (2015) solved the problem of steady boundary layer flow of a nanofluid past a permeable exponentially shrinking surface with convective surface condition using Buongiorno's model.

Besides Fang *et al*. (2009), all studies mentioned above considered the steady state problem, where the velocity and other properties such as pressure at every point do not depend upon time. Steady flow is preferred by engineers because it is easier to control. However, the study of unsteady boundary layer flow is much more important, because all boundary layer problems that occur in real-world practice are depending on time. Surma Devi *et al*. (1986) discussed the flow, heat and species transport due to the unsteady, three-dimensional flow caused the stretching of a flat surface. Wang (1989) investigated the exact solutions of the unsteady Navier-Stokes equation. The unsteady boundary layer flow due to a stretching surface in a rotating fluid has been studied by Nazar *et al*. (2004). Very recently, Roşca and Pop (2015) investigated the unsteady viscous flow over a curved stretching/shrinking surface with mass suction.

The purpose of this paper is to study the boundary layer flow due to the unsteady, three-dimensional laminar flow of a viscous fluid over a permeable stretching/shrinking sheet. The governing partial differential equations are transformed into a system of ordinary differential equations by using an appropriate similarity transformation, and then solved numerically with "bvp4c" function in MATLAB. Stability analysis is performed to determine the stability of the multiple solutions obtained.

2. Governing Equations

We consider the unsteady three-dimensional boundary layer flow of a viscous fluid past a permeable stretching/shrinking flat surface. A set of coordinates (x, y, z) is measured normal to the sheet. The *x*- and *y*-coordinates are in the plane of the sheet, while the *z*-coordinate is perpendicularly measured to the shrinking surface. We assume that the flat surface is stretching/shrinking continuously in both *x*- and *y*-directions with the velocities $u(x,t) = u_w(x,t)$ and $v(y,t) = v_w(y,t)$, respectively. The mass flux velocity is written as $w = w_0(t)$, where $w_0(t) < 0$ is for suction and $w_0(t) > 0$ is for injection or withdrawal of the fluid. Under these assumptions and conditions, the governing boundary layer equations can be expressed as (see Surma Devi *et al*. (1986))

$$\frac{\partial u}{\partial x}+\frac{\partial v}{\partial y}+\frac{\partial w}{\partial z}=0, \tag{1}$$

$$\frac{\partial u}{\partial t}+u\frac{\partial u}{\partial x}+v\frac{\partial u}{\partial y}+w\frac{\partial u}{\partial z}=\nu\frac{\partial^2 u}{\partial z^2}, \tag{2}$$

$$\frac{\partial v}{\partial t}+u\frac{\partial v}{\partial x}+v\frac{\partial v}{\partial y}+w\frac{\partial v}{\partial z}=\nu\frac{\partial^2 v}{\partial z^2}, \tag{3}$$

subject to the following initial and boundary conditions:

$$\begin{aligned} &t<0:\; u(x,y,z)=0,\; v(x,y,z)=0,\; w(x,y,z)=0 \text{ for any } x,\; y,\; z,\\ &t\ge 0:\; u=u_w(x,t)=\frac{\lambda a x}{1-\beta t},\; v=v_w(y,t)=\frac{\lambda b y}{1-\beta t},\; w(t)=\frac{w_0}{\sqrt{1-\beta t}} \text{ at } z=0,\\ &\qquad u(x,y,z)\to 0,\; v(x,y,z)\to 0,\; w(x,y,z)\to 0 \text{ as } z\to\infty, \end{aligned} \tag{4}$$

where u, v and w are the velocity components along the x-, y- and z-axes, respectively, a and b are positive constants, t is the time, β is the parameter showing the unsteadiness of the problem, ν is the kinematic viscosity of the fluid and λ is the stretching ($\lambda > 0$) or shrinking parameter ($\lambda < 0$).

We now introduce the following similarity variables:

$$\begin{aligned} &u=\frac{a\,x}{1-\beta t}f'(\eta),\;\; v=\frac{b\,y}{1-\beta t}g'(\eta),\;\; w=-\sqrt{\frac{a\nu}{1-\beta t}}\left(f(\eta)+\kappa g(\eta)\right),\\ &\eta=\sqrt{\frac{a/\nu}{1-\beta t}}\,z, \end{aligned} \tag{5}$$

where primes denote the differentiation with respect to η and $\kappa = b/a$ is the ratio of the surface velocity gradients along the y- and x-directions. Using the similarity variables (5), (1) is automatically satisfied, while Eqs. (2) and (3) are reduced to the following system of ordinary differential equations

$$f'''+\left(f+\kappa g\right)f''-f'^2-M\left(f'+\frac{\eta}{2}f''\right)=0, \tag{6}$$

$$g'''+\left(f+\kappa g\right)g''-\kappa g'^2-M\left(g'+\frac{\eta}{2}g''\right)=0, \tag{7}$$

and the boundary conditions (4) are reduced to

$$\begin{aligned} &f(0)=S,\; g(0)=0,\; f'(0)=\lambda,\; g'(0)=\lambda,\\ &f'(\eta)\to 0,\; g'(\eta)=0 \text{ as } \eta\to\infty, \end{aligned} \tag{8}$$

where $M=\beta/a$ is the unsteadiness parameter and $S=-w_0(t)(1-\beta t)/(a\nu)^{1/2}$ is the surface mass transfer parameter with $S>0$ for suction and $S<0$ for injection. In this paper, we confine our attention here only to the case when $\kappa=0.5$ and $M<0$ (decelerated flow).

The quantities of physical interest are the local skin friction coefficients C_{fx} and C_{fy}, which are defined as

$$C_{fx} = \frac{2\tau_{wx}}{\rho u_w^2}, \ C_{fy} = \frac{2\tau_{wy}}{\rho v_w^2}, \tag{9}$$

where τ_{wx} and τ_{wy} are the shear stresses in the x- and y-directions of the sheet, which are given by

$$\tau_{wx} = \mu\left(\frac{\partial u}{\partial z}\right)_{z=0}, \ \tau_{wy} = \mu\left(\frac{\partial v}{\partial z}\right)_{z=0}. \tag{10}$$

Substituting (5) into (10) and using Eq. (9), we obtain

$$\mathrm{Re}_x^{1/2}\, C_{fx} = 2f''(0), \ \ \mathrm{Re}_y^{1/2}\, C_{fy} = 2g''(0), \tag{11}$$

where $\mathrm{Re}_x = u_w(x,t)x/\nu_f$ and $\mathrm{Re}_y = v_w(y,t)y/\nu_f$ are the local Reynolds numbers based on the velocities $u_w(x,t)$ and $v_w(y,t)$, respectively.

3. Stability Analysis

In the introduction section, we have mentioned the existence of dual solutions, which are categorised as upper branch for first solution, and lower branch for second solution. Weidman *et al*. (2006) and Roşca and Pop (2013) have shown in their papers that the second (lower branch) solutions are unstable, while the first (upper branch) solutions are stable and physically realisable. The stability of both branches can be determined by performing a stability analysis. This analysis has also been done by previous researchers, such as Merkin (1986), Weidman and Sprague (2011), Mahapatra and Nandy (2011), Nazar *et al*. (2014) and others.

Following Weidman *et al*. (2006), a new dimensionless time variable τ is introduced. The use of τ is associated with an initial value problem and is consistent with the question of which solution or branch will be obtained in practice (physically realisable).

With the introduction of τ and (5), we have

$$\begin{gathered} u = \frac{a\,x}{1-\beta t} f'(\eta,\tau), \ \ v = \frac{b\,y}{1-\beta t} g'(\eta,\tau), \ \ w = -\sqrt{\frac{a\nu}{1-\beta t}}\big(f(\eta,\tau) + cg(\eta,\tau)\big), \\ \eta = \sqrt{\frac{a/\nu}{1-\beta t}}\, z, \ \ \tau = \frac{a\,t}{1-\beta t}. \end{gathered} \tag{12}$$

Substituting (12) into (2) and (3), we obtain the following:

$$\frac{\partial^3 f}{\partial \eta^3} + (f + \kappa g)\frac{\partial^2 f}{\partial \eta^2} - \left(\frac{\partial f}{\partial \eta}\right)^2 - M\left(\frac{\partial f}{\partial \eta} + \frac{\eta}{2}\frac{\partial^2 f}{\partial \eta^2}\right) - \frac{1}{1-\beta t}\frac{\partial^2 f}{\partial \eta\, \partial \tau} = 0, \tag{13}$$

$$\frac{\partial^3 g}{\partial \eta^3} + (f + \kappa g)\frac{\partial^2 g}{\partial \eta^2} - \kappa\left(\frac{\partial g}{\partial \eta}\right)^2 - M\left(\frac{\partial g}{\partial \eta} + \frac{\eta}{2}\frac{\partial^2 g}{\partial \eta^2}\right) - \frac{1}{1-\beta t}\frac{\partial^2 g}{\partial \eta\, \partial \tau} = 0, \tag{14}$$

subject to the boundary conditions

$$\begin{gathered} f(0,\tau)=S,\ \ g(0,\tau)=0,\ \frac{\partial f}{\partial \eta}(0,\tau)=\lambda,\ \ \frac{\partial g}{\partial \eta}(0,\tau)=\lambda, \\ \frac{\partial f}{\partial \eta}(\eta,\tau)\to 0,\ \ \ \frac{\partial g}{\partial \eta}(\eta,\tau)\to 0 \quad \text{as } \eta\to\infty. \end{gathered} \tag{15}$$

To test the stability of the solution $f(\eta)=f_0(\eta)$ and $g(\eta)=g_0(\eta)$ satisfying the boundary-value problem (6)-(8), we write (see Weidman *et al*. (2006) and Roşca and Pop (2013))

$$f(\eta,\tau)=f_0(\eta)\ +\ e^{-\sigma\tau}F(\eta,\tau),\ \ g(\eta,\tau)=g_0(\eta)\ +\ e^{-\sigma\tau}G(\eta,\tau), \tag{16}$$

where σ is an unknown eigenvalue parameter, and $F(\eta,\tau)$ and $G(\eta,\tau)$ are small relative to $f_0(\eta)$ and $g_0(\eta)$.
Substituting (16) into Eqs. (13) and (14), we obtain the following linearised problem:

$$\begin{aligned} &\frac{\partial^3 F}{\partial \eta^3}+\left(f_0+\kappa g_0\right)\frac{\partial^2 F}{\partial \eta^2}+\left(F+\kappa G\right)f_0''-\left(2f_0'-\left(1+M\tau\right)\sigma\right)\frac{\partial F}{\partial \eta} \\ &\qquad -M\left(\frac{\partial F}{\partial \eta}-\frac{\eta}{2}\frac{\partial^2 F}{\partial \eta^2}\right)-\left(1+M\tau\right)\frac{\partial^2 F}{\partial \eta \partial \tau}=0, \end{aligned} \tag{17}$$

$$\begin{aligned} &\frac{\partial^3 G}{\partial \eta^3}+\left(f_0+\kappa g_0\right)\frac{\partial^2 G}{\partial \eta^2}+\left(F+\kappa G\right)g''-\left(2\kappa g_0'-\left(1+M\tau\right)\sigma\right)\frac{\partial G}{\partial \eta} \\ &\qquad -M\left(\frac{\partial G}{\partial \eta}+\frac{\eta}{2}\frac{\partial^2 G}{\partial \eta^2}\right)-\left(1+M\tau\right)\frac{\partial^2 G}{\partial \eta \partial \tau}=0, \end{aligned} \tag{18}$$

subject to the boundary conditions

$$\begin{gathered} F(0,\tau)=S,\ \ G(0,\tau)=0,\ \frac{\partial F}{\partial \eta}(0,\tau)=\lambda,\ \ \frac{\partial G}{\partial \eta}(0,\tau)=\lambda, \\ \frac{\partial F}{\partial \eta}(\eta,\tau)\to 0,\ \ \ \frac{\partial G}{\partial \eta}(\eta,\tau)\to 0 \quad \text{as} \quad \eta\to\infty. \end{gathered} \tag{19}$$

As suggested by Weidman *et al*. (2006), we investigate the stability of the steady flow $f_0(\eta)$ and $g_0(\eta)$ by setting $\tau=0$. Hence, $F(\eta)=F_0(\eta)$ and $G(\eta)=G_0(\eta)$ in Eqs. (17) and (18) identify the initial growth or decay of the solution (16). To test our numerical procedure, we have to solve the linear eigenvalue problem

$$F_0'''+\left(f_0+\kappa g_0\right)F_0''+\left(F_0+\kappa G_0\right)f_0''-\left(2f_0'-\sigma\right)F_0'-M\left(F_0'-\frac{\eta}{2}F_0''\right)=0, \tag{20}$$

$$G_0'''+\left(f_0+\kappa g_0\right)G_0''+\left(F_0+\kappa G_0\right)g_0''-\left(2\kappa g_0'-\sigma\right)G_0'-M\left(G_0'+\frac{\eta}{2}G_0''\right)=0, \tag{21}$$

along with the following boundary conditions:

$$F_0(0)=0,\;\; F_0'(0)=0,\;\; G_0(0)=0,\;\; G_0'(0)=0, \\ F_0'(\eta)\to 0,\;\; G_0(\eta)\to 0 \;\text{ as }\; \eta\to\infty. \tag{22}$$

For particular values of the governing parameters involved, such as *M*, *S* and *λ*, the stability of the corresponding steady flow solution $f_0(\eta)$ and $g_0(\eta)$ are determined by the smallest eigenvalue σ. Solutions of the linear eigenvalue problem (20) and (21) give an infinite set of eigenvalues $\sigma_1<\sigma_2<\sigma_3<\ldots;$ if the smallest eigenvalue σ_1 is positive $(\sigma_1\geq 0)$, then there is an initial decay of disturbances and the flow is stable, and if σ_1 is negative $(\sigma_1<0)$, then there is an initial growth of disturbances, which indicates that the flow is unstable. Harris *et al*. (2009) suggested that the range of possible eigenvalues can be obtained by relaxing a boundary condition on $F_0(\eta)$ or $G_0(\eta)$. In this paper, we relax the condition $G_0'(\eta)\to 0$ as $\eta\to\infty$ and for a fixed value of *σ*, we solve the system of equations (20) and (21) subject to the boundary conditions (22), along with the new boundary condition $G_0''(0)=1$.

4. Results and Discussion

The system of nonlinear ordinary differential equations (6) and (7) subject to the boundary conditions (8) are solved numerically using the "bvp4c" function in MATLAB. This function has been introduced by Kierzenka and Shampine (2001) and Shampine *et al*. (2003) to solve a two-point boundary value problem for ordinary differential equations. The numerical results for the reduced skin friction coefficients obtained in this study are compared with those of Surma Devi *et al*. (1986) for validation. The comparisons, which are displayed in Table 1, are found to be in excellent agreement, and thus we are confident that the present numerical method is accurate.

Table 1: Numerical comparison with those of Surma Devi *et al*. (1986) by setting the following parameters: $\kappa=1,\, S=0$ and boundary conditions $f'(0)=1,\; g'(0)=0.5$

	Surma Devi *et al*. (1986)		Present study	
M	$-f''(0)$	$-g''(0)$	$-f''(0)$	$-g''(0)$
1	1.3814	0.6261	1.3814	0.6261
0.5	1.2407	0.5480	1.2407	0.5480
0	1.0931	0.4652	1.0931	0.4652
-0.5	0.9430	0.3809	0.9430	0.3809
-1	0.7912	0.2956	0.7912	0.2956

Dual solutions in this study are obtained by setting 2 different initial guesses for the missing values of $f''(0)$ and $g''(0)$. Table 2 displays both first (upper branch) and second (lower branch) solutions of $f''(0)$ and $g''(0)$ for different values of *M* when $S=2.5,\ \lambda=-1$ and $c=0.5$. From the table, it can be observed that the values of $f''(0)$ and $g''(0)$ from the upper branch are decreasing with the decrease of *M*, up until they have reached zero and become negative. This implies that there is a velocity overshoot near the shrinking sheet with a higher velocity in the fluid than the wall velocity (Fang *et al*. (2009)). Meanwhile, different behaviour can be seen for the lower branch, where the values keep decreasing, and then increasing as *M* is getting closer to M_c, where M_c is a critical value of *M*. These kind of behaviour can also be seen in Figures 1 and 2. These figures also show that the solutions of $f''(0)$ and $g''(0)$ can be positive for both branches when the value of suction parameter *S* is small $(S < 2.4)$. Furthermore, it can also be seen that the solutions keep decreasing with the decrease of *M* and *S*.

Table 2: Dual solutions of $f''(0)$ and $g''(0)$ for different values of *M* when $S = 2.5$, $\lambda = -1$ and $c = 0.5$

	Upper branch		Lower branch	
M	$f''(0)$	$g''(0)$	$f''(0)$	$g''(0)$
0	1.7824	1.9493	0.8315	1.6452
-2	0.9787	1.2405	-0.5351	0.5270
-4	0.1010	0.4846	-1.4710	-0.3242
-6	-0.8830	-0.3362	-2.1985	-1.0453
-8	-2.2062	-1.3536	-2.5299	-1.5334
-8.1	-2.3969	-1.4741	-2.4212	-1.4876
-8.1008 (=M_c)	-2.4064	-1.4795	-2.4117	-1.4825

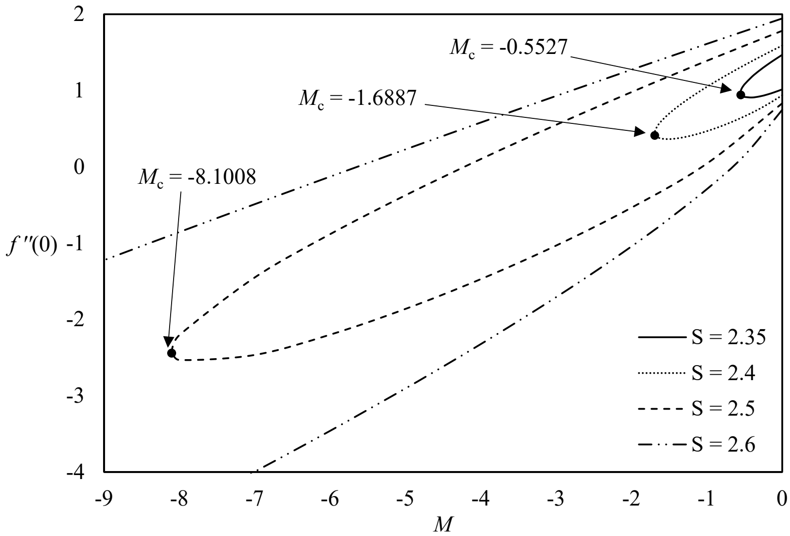

Figure 1: Variation of $f''(0)$ with *M* for different values of *S* when $c = 0.5$ and $\lambda = -1$

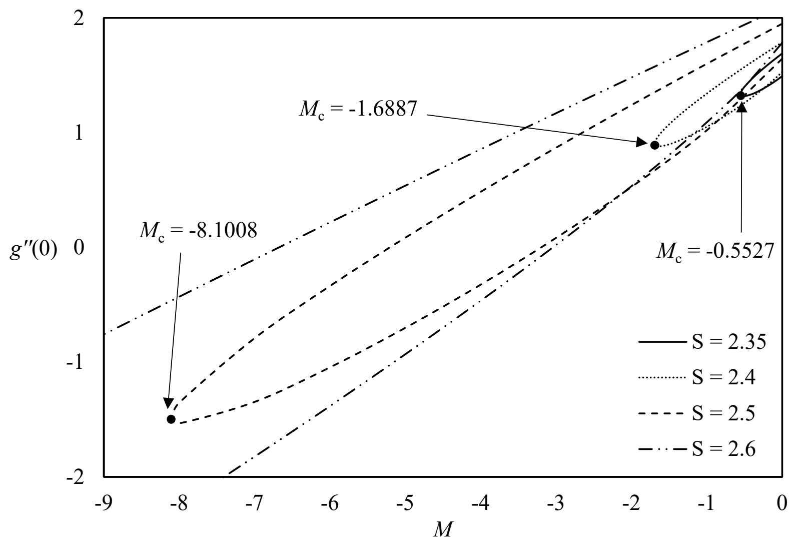

Figure 2: Variation of $g''(0)$ with *M* for different values of *S* when $c = 0.5$ and $\lambda = -1$

Table 3: Dual solutions of $f''(0)$ and $g''(0)$ for different values of *M*, *S* and *λ* when $c = 0.5$

			Upper branch		Lower branch	
λ	*M*	*S*	$f''(0)$	$g''(0)$	$f''(0)$	$g''(0)$
1	-1	2.5	-2.7666	-2.6816	-7.8187	-2.1881
		3	-3.2295	-3.1555	-10.1723	-2.6553
		4	-4.1783	-4.1201	-16.4292	-3.5998
	-3	2.5	-2.4512	-2.3578	-11.8784	-1.1936
		3	-2.9505	-2.8708	-15.1199	-1.7673
		4	-3.9541	-3.8930	-23.5231	-2.8671
-1	-1	2.5	1.3891	1.6004	0.0426	1.0214
		3	2.2626	2.3825	-1.6230	1.6047
		4	3.5113	3.5852	-6.0139	2.8919
	-3	2.5	0.5502	0.8690	-1.0313	0.0835
		3	1.8005	1.9423	-4.0940	0.4530
		4	3.2210	3.3007	-11.0877	1.9915

Figures 1-4 represent the solution domain for Eqs. (6) and (7) with boundary conditions (8). From these figures, it can be seen that there are two (dual) solutions for each $f''(0)$ and $g''(0)$, and they exist for a certain range of *M* and *λ*. When *M* and *λ* equal to a certain value, say $M = M_c$ and $\lambda = \lambda_c$, where M_c and λ_c are the critical values of *M* and *λ*, respectively, there is only one solution. There is no solution when the values of *M* and *λ* are less than their critical values, beyond which the boundary layer separates from the surface (which is known as boundary layer separation) and the solution based upon the boundary layer approximations are not possible. From these figures, we notice that the upper branch solutions are always larger than the lower branch solutions for the same value of M and λ, which is consistent with the numerical results displayed in Tables 2 and 3.

Meanwhile, Table 3 displays both solutions of $f''(0)$ and $g''(0)$ for different values of M, S and λ when $c = 0.5$. It can be seen that the magnitude of solutions increase with the increase of S and decrease with the increase of $|M|$. Table 3 also shows that dual solutions exist for both stretching and shrinking cases. This behaviour is also displayed in Figures 3 and 4, which illustrate the variation of $f''(0)$ and $g''(0)$ with λ for different values of M when $c = 0.5$ and $S = 3$. These figures also show that the values of $|\lambda_c|$ increase with the decrease of $|M|$.

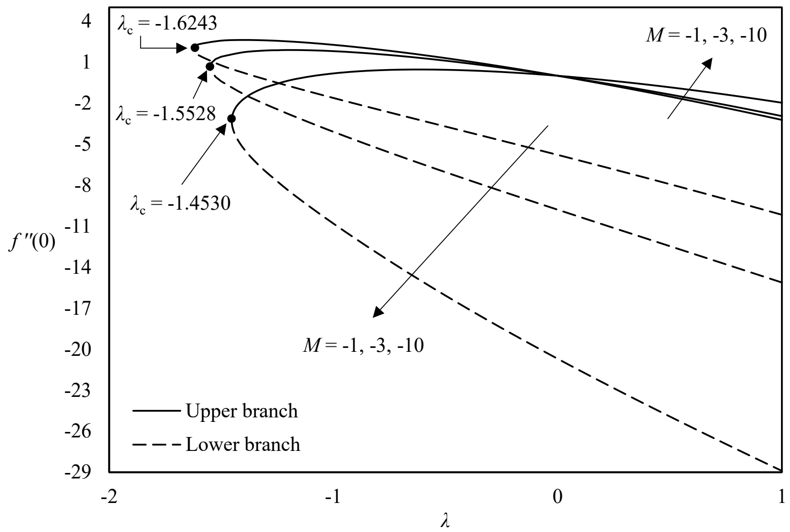

Figure 3: Variation of $f''(0)$ with λ for different values of M when $c = 0.5$ and $S = 3$

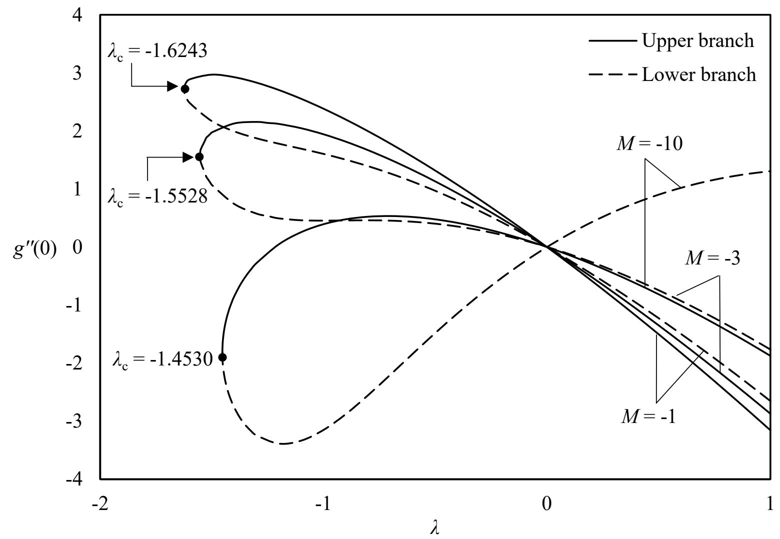

Figure 4: Variation of $g''(0)$ with λ for different values of M when $c = 0.5$ and $S = 3$

Table 4 displays the critical values of $S\left(=S_c\right)$ for several values of *M* when $c=0.5$ and $\lambda=-1$. We found that the values of S_c increase with the increase of $|M|$. Together with Figures 3 and 4, we can conclude that the unsteadiness parameter *M* widen the range of *λ* and *S* for which solutions exist. Further, the velocity profiles $f'(\eta)$ and $g'(\eta)$ for some values of *S* when $M=-1$, $\lambda=-1$ and $c=0.5$ are illustrated in Figures 5 and 6, respectively. The boundary layer thicknesses from both figures are seen to be smaller with higher values of *S*, which happened because suction reduces drag force to avoid boundary layer separation. We also notice that the boundary layer thickness for the lower branch solution is larger than the upper branch solution. Both of these profiles satisfy the far field boundary conditions (8) asymptotically, which support the validity of the numerical results obtained and the existence of the dual solutions shown in Figures 1-4 and Tables 1-3.

Table 4: Values of S_c for several values of *M* when $c=0.5$ and $\lambda=-1$

M	S_c
0	2.3014
-1	2.3738
-3	2.4338
-10	2.5147

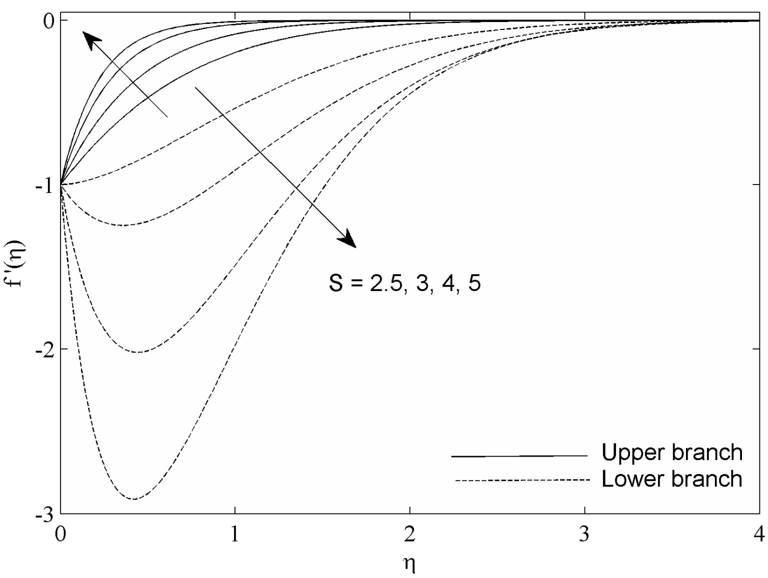

Figure 5: Velocity profiles $f'(\eta)$ for different values of *S* when $M=-1$, $c=0.5$ and $\lambda=-1$

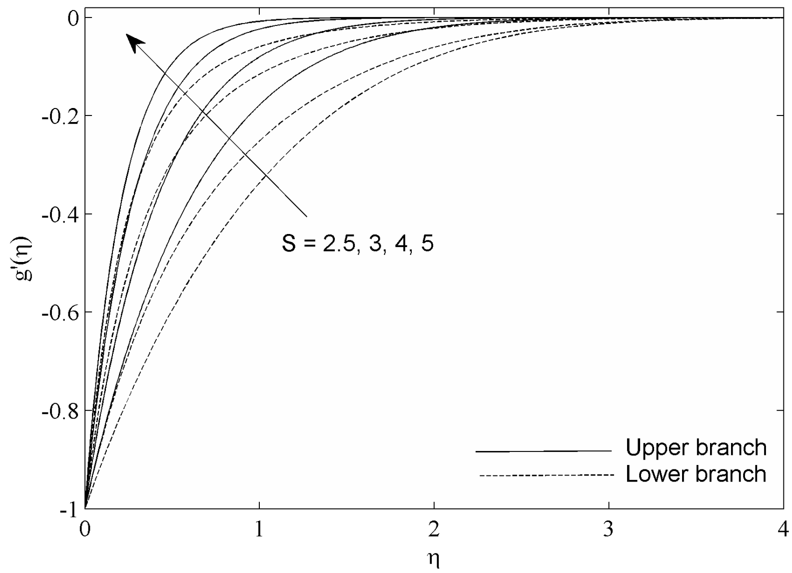

Figure 6: Velocity profiles $g'(\eta)$ for different values of *S* when $M = -1,\ c = 0.5$ and $\lambda = -1$

To determine the stability of the dual solutions obtained, a stability analysis is performed by determining an unknown eigenvalue σ on Eqs. (20) and (21) along with the boundary conditions (22). This analysis has been done by using the same numerical computation used in this study, which is the "bvp4c" function. The smallest eigenvalues σ for some values of *M* and *S* when $c = 0.5$ and $\lambda = -1$ are presented in Table 5. From the table, it can be observed that the upper branch solutions have positive eigenvalues σ while the lower branch solutions have negative eigenvalues σ. Thus, we conclude that the first (upper branch) solution is stable and physically realisable while the second (lower branch) solution is not.

Table 5: Smallest eigenvalues σ for several values of *M* and *S* when $c = 0.5$ and $\lambda = -1$

M	*S*	*σ (upper branch)*	*σ (lower branch)*
-1	2.38	0.1675	-0.1617
	2.4	0.3514	-0.3270
	2.5	0.8194	-0.7028
-3	2.44	0.2415	-0.2358
	2.5	0.8146	-0.7548
	2.6	1.3421	-1.1924
-10	2.52	0.3617	-0.3569
	2.55	0.9406	-0.9091
	2.6	1.4857	-1.4097

5. Conclusions

We have studied the problem of unsteady three-dimensional boundary layer flow of a viscous fluid past a permeable stretching/shrinking sheet. The governing system of nonlinear partial differential equations is reduced to a system of ordinary differential equations by using similarity transformation, and then solved numerically using the "bvp4c" function in

MATLAB. A comparison has been made with previous literature and it shows an excellent agreement. Dual solutions are found for both stretching and shrinking cases when the suction parameter $S > 2$. The solutions for lower branch are always smaller than the upper branch. The magnitude of reduced skin friction coefficients are found to increase with the increase of the suction parameter and the decrease of the unsteadiness parameter. The boundary layer thicknesses are seen to be smaller with higher values of the suction parameter. A stability analysis has been performed to determine the stability of the dual solutions obtained, and it can be concluded that the first (upper branch) solution is stable and physically realisable, while the second (lower branch) solution is unstable.

Acknowledgements

This work was supported by a research grant (Project Code: GUP-2013-040) from the Universiti Kebangsaan Malaysia.

References

Aman F. & Ishak A. 2010. Boundary layer flow and heat transfer over a permeable shrinking sheet with partial slip. *Journal of Applied Sciences Research* **6**(8): 1111–1115.

Banks W.H.H. 1983. Similarity solutions of the boundary-layer equations for a stretching wall. *Journal de Mecanique Theorique et Appliquee* **2**: 375–392.

Bhattacharyya K. & Layek G.C. 2014. Magnetohydrodynamic boundary layer flow of nanofluid over an exponentially stretching permeable sheet. *Physics Research International* **2014**: 1–12.

Chen C-K. & Char M-I. 1988. Heat transfer of a continuous, stretching surface with suction or blowing. *Journal of Mathematical Analysis and Applications* **135**(2): 568–580.

Crane L.J. 1970. Flow past a stretching plate. *Zeitschrift für angewandte Mathematik und Physik* **21**(4): 645–647.

Fang T-G., Zhang J. & Yao S.-S. 2009. Viscous flow over an unsteady shrinking sheet with mass transfer. *Chinese Physics Letters* **26**(1): 014703.

Goldstein S. 2006. On backward boundary layers and flow in converging passages. *Journal of Fluid Mechanics* **21**(1): 33–45.

Gupta P.S. & Gupta A.S. 1977. Heat and mass transfer on a stretching sheet with suction or blowing. *Canadian Journal of Chemical Engineering* **55**: 744–746.

Harris S.D., Ingham D.B. & Pop I. 2009. Mixed convection boundary-layer flow near the stagnation point on a vertical surface in a porous medium: Brinkman model with slip. *Transport in Porous Media* **77**(2): 267–285.

Hayat T., Abbas Z., Javed T. & Sajid M. 2009. Three-dimensional rotating flow induced by a shrinking sheet for suction. *Chaos, Solitons & Fractals* **39**(4): 1615–1626.

Kierzenka J. & Shampine L.F. 2001. A BVP solver based on residual control and the Maltab PSE. *ACM Transactions on Mathematical Software* **27**(3): 299–316.

Mabood F., Khan W.A. & Ismail A.I.M. 2015. MHD boundary layer flow and heat transfer of nanofluids over a nonlinear stretching sheet: A numerical study. *Journal of Magnetism and Magnetic Materials* **374**: 569–576.

Magyari E. & Keller B. 1999. Heat and mass transfer in the boundary layers on an exponentially stretching continuous surface. *Journal of Physics D: Applied Physics* **32**(5): 577–585.

Magyari E. & Keller B. 2000. Exact solutions for self-similar boundary-layer flows induced by permeable stretching walls. *European Journal of Mechanics - B/Fluids* **19**(1): 109–122.

Mahapatra T.R. & Nandy S.K. 2011. Stability analysis of dual solutions in stagnation-point flow and heat transfer over a Power-law shrinking surface. *International Journal of Nonlinear Science* **12**: 86–94.

McLeod J.B. & Rajagopal K.R. 1987. On the uniqueness of flow of a Navier-Stokes fluid due to a stretching boundary. *Archive for Rational Mechanics and Analysis* **98**(4): 385–393.

Merkin J.H. 1986. On dual solutions occurring in mixed convection in a porous medium. *Journal of Engineering Mathematics* **20**(2): 171–179.

Miklavcic M. & Wang C.Y. 2006. Viscous flow due to a shrinking sheet. *Quarterly of Applied Mathematics* **64**: 283–290.

Nadeem S., Haq R.U. & Khan Z. 2014. Numerical study of MHD boundary layer flow of a Maxwell fluid past a stretching sheet in the presence of nanoparticles. *Journal of the Taiwan Institute of Chemical Engineers* **45**(1): 121–126.

Nazar R., Amin N. & Pop I. 2004. Unsteady boundary layer flow due to a stretching surface in a rotating fluid. *Mechanics Research Communications* **31**(1): 121–128.
Nazar R., Noor A., Jafar K. & Pop I. 2014. Stability analysis of three-dimensional flow and heat transfer over a permeable shrinking surface in a Cu-water nanofluid. *International Journal of Mathematical, Computational, Physical and Quantum Engineering* **8**(5): 776–782.
Rahman M.M., Rosca A.V. & Pop I. 2015. Boundary layer flow of a nanofluid past a permeable exponentially shrinking surface with convective boundary condition using Buongiorno's model. *International Journal of Numerical Methods for Heat and Fluid Flow* **25**(2): 299–319.
Rajagopal K.R., Na T.Y. & Gupta A.S. 1984. Flow of a viscoelastic fluid over a stretching sheet. *Rheologica Acta* **23**: 213–215.
Rohni A.M., Ahmad S. & Pop I. 2014. Flow and heat transfer at a stagnation-point over an exponentially shrinking vertical sheet with suction. *International Journal of Thermal Sciences* **75**: 164–170.
Roşca A.V. & Pop I. 2013. Flow and heat transfer over a vertical permeable stretching/shrinking sheet with a second order slip. *International Journal of Heat and Mass Transfer* **60**: 355–364.
Roşca N.C. & Pop I. 2015. Unsteady boundary layer flow over a permeable curved stretching/shrinking surface. *European Journal of Mechanics - B/Fluids* **51**: 61–67.
Sakiadis B. 1961a. Boundary-layer behavior on continuous solid surfaces: I. Boundary-layer equations for two-dimensional and axisymmetric flow. *AIChE Journal* **7**: 26–28.
Sakiadis B. 1961b. Boundary-layer behavior on continuous solid surfaces: II. The boundary layer on a continuous flat surface. *AIChE Journal* **7**(2): 221–225.
Shampine L.F., Gladwell I. & Thompson S. 2003. *Solving ODEs with MATLAB.* Cambridge University Press.
Surma Devi C.D., Takhar H.S. & Nath G. 1986. Unsteady, three-dimensional, boundary-layer flow due to a stretching surface. *International Journal of Heat and Mass Transfer* **29**(12): 1996–1999.
Tsou F.K., Sparrow E.M. & Goldstein R.J. 1967. Flow and heat transfer in the boundary layer on a continuous moving surfaces. *International Journal of Heat and Mass Transfer* **10**: 219–235.
Wang C.Y. 1984. The three-dimensional flow due to a stretching flat surface. *Physics of Fluids* **27**(8): 1915–1917.
Wang C.Y. 1989. Exact solutions of the unsteady Navier-Stokes equations. *Applied Mechanics Reviews* **42**(11S): S269–S282.
Weidman P.D., Kubitschek D.G. & Davis A.M.J. 2006. The effect of transpiration on self-similar boundary layer flow over moving surfaces. *International Journal of Engineering Science* **44**(11-12): 730–737.
Weidman P.D. & Sprague M.A. 2011. Flows induced by a plate moving normal to stagnation-point flow. *Acta Mechanica* **219**(3-4): 219–229.

[1]*School of Mathematical Sciences*
Faculty of Science & Technology
Universiti Kebangsaan Malaysia
43600 UKM Bangi
Selangor DE, MALAYSIA
E-mail: ezadhafidz@gmail.com, rmn@ukm.edu.my[*]

[2]*Department of Mathematics*
Universiti Putra Malaysia
43400 UPM Serdang,
Selangor DE, MALAYSIA
E-mail: norihanarifin@yahoo.com

[3]*Department of Mathematics*
Babeş-Bolyai University
R-400048 Cluj-Napoca
ROMANIA
E-mail: popm.ioan@yahoo.co.uk

[*]Corresponding author